The effect of temperature on the resonant tunneling and electric field domain formation in multiple quantum well superlattices

Yuanjian Xu,[a] Ali Shakouri, and Amnon Yariv
Department of Applied Physics 128-95, California Institute of Technology, Pasadena, California 91125

(Received 23 September 1996; accepted for publication 12 November 1996)

Analyzing the photocurrent spectra and the $I-V$ characteristics of weakly coupled GaAs/AlGaAs multiquantum well structures, different transport regimes are distinguished. At low temperatures (below ~50 K), due to the electron coherence over a few periods of the superlattice, electron transport is dominated by sequential resonant tunneling. At higher temperatures, evidences for the increased contribution of nonresonant transport processes, and the subsequent modification in the electric field distribution in the device, are presented. © *1997 American Institute of Physics.* [S0021-8979(97)04504-0]

Electron transport in multiple quantum well (MQW) superlattices is dominated by sequential resonant tunneling when resonant coupling between adjacent wells exists. This is the origin of a negative differential resistance mechanism whose attendant instabilities give rise to electric field domain (EFD) formation in the MQW region.[1–3] Esaki and Chang[1] first studied this effect in a strongly coupled MQW structure. They observed discontinuities in the $I-V$ characteristics with an average separation equal to the subband spacings (in volts) in each quantum well (QW).[1,3] This was explained through the formation of high and low EFDs in the structure and the stepwise increase in the high field domain (HFD) size with increasing external bias.

Even though it is the electron coherence over distances of at least the order of neighboring well separation which is the origin of resonant tunneling, it is difficult to directly relate the dc transport experiments to the electron coherence length. Recently, the sensitivity of the photocurrent spectra in single-bound state MQW structures to well spacings and to the electric field was used to investigate electron coherence effects and the electric field distribution in the device.[4] In this letter, we report on the effect of the temperature on current transport in MQW devices, showing how the transport changes from being dominated by sequential resonant tunneling at low temperatures to domination by nonresonant processes at higher temperatures. Evidences for these nonresonant transport mechanisms which lead to strong changes in the electric field distribution in the device are also presented.

The sample used for this study was grown by molecular beam epitaxy on a (100) semi-insulating GaAs substrate. It consists of 50 periods of 4 nm GaAs wells, uniformly doped with Si to $n=2\times10^{18}$ cm^{-3}, separated by 20 nm $Al_{0.22}Ga_{0.78}As$ barriers. As discussed in Ref. 4, the sample was designed to have one bound state in the well, and a first resonant state highly in the continuum, about 24 meV above the barrier. Devices with 200 μm diameter were fabricated by standard photolithography and wet chemical etching techniques. The peak at ~155 meV in the photocurrent spectrum at $V_{bias}=-2$ V and $T=10$ K, as shown in Fig. 1(a), corresponds to the transition from the ground state to the first continuum resonant state of an isolated QW. The auxiliary peak at ~187 meV is due to electron interference effects over a few superlattice periods. The sample manifested the same peaks at all biases between −0.3 and −4.3 V. This is explained through the formation of EFDs in the superlattice because the main contribution to the photocurrent comes from photoexcited carriers in the HFD. Increasing the external bias increases the size of the HFD, but it does not change the strength of HFD electric field, and so the shape of the photoresponse spectrum is not modified significantly. The calculated absorption spectrum based on the self-consistent solution of the Schrödinger and Poisson equations is shown in Fig. 1(b).[4] Assuming electron coherence length of a few periods of the superlattice and an electric field strength of ~31 kV/cm in the HFD, one can deduce the positions of the peaks in good agreement with the experimental photocurrent spectrum.

The current–voltage characteristics are shown in Fig. 2. The low temperature oscillatory behavior, which is better shown in Fig. 3, is more evidence for the existence of EFDs in the superlattice.[4] Figure 3 shows also the sweep-up and the sweep-down measurements of the $I-V$ characteristics, which supports the multistability observation of Ref. 5, and is an indication of the complexity of the growth of electric field domains in the device.[6]

As long as incoherent transport processes (such as thermionic emission or nonresonant tunneling) are not dominating the current, it should be possible to observe sequential resonant tunneling and electric field domain formation at higher temperatures. The measured photocurrent spectrum at $T=50$ K [see Fig. 1(a)] had a main peak at ~150 meV, corresponding to the intersubband transition from the ground state to the first resonant state. The small redshift of the peak position relative to that at $T=10$ K can be explained by a reduction of the electric field strength in the HFD because the effective mass and the conduction band offset temperature dependencies can be neglected in this temperature range.[7] The self-consistent simulation gives an electric field strength of ~26 kV/cm in the HFD. One also notices the presence of side peak at ~182 meV in the photocurrent spectrum at $T=50$ K. This peak, being an indication of electron coherence over the QW structure,[4] is, however, less pro-

[a]Electronic mail: yjxu@cco.caltech.edu

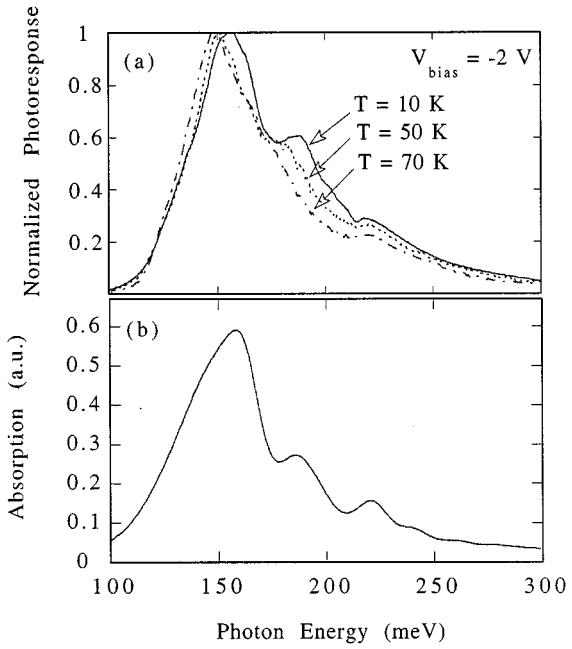

FIG. 1. (a) Experimental photoresponse spectra at $V_{\text{bias}}=-2$ V (defined with respect to the bottom contact) for different temperatures; solid line: $T=10$ K, dashed line: $T=50$ K, dash-dotted line: $T=70$ K. (b) Theoretical absorption spectrum for two superlattice periods at $T=10$ K and assumed $F=-31$ kV/cm.

nounced than the 10 K one. This suggests an increased contribution of incoherent processes to the photocurrent spectrum at higher temperatures. The reduction of electric field might also contribute to this observation (the resonance state is less localized for smaller electric field). The oscillations in the 50 K $I-V$ characteristics show the still dominant EFD formation in the device.

At a temperature of 70 K, the side peak at ~182 meV is almost invisible [see Fig. 1(a)]. This implies a possible shortening of the electron coherence length and/or electric field nonuniformity due to the fact that the three dimensional (3D) cathode has to provide large 2D current in the superlattice.[8] In contrast to intersubband transitions between bound states, these bound-to-continuum transitions are very sensitive to

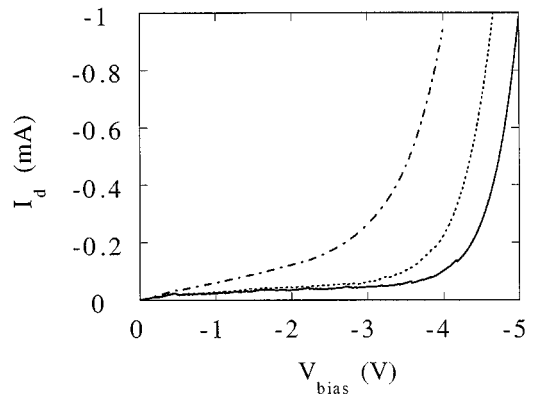

FIG. 2. Dark current–voltage characteristics for different temperatures; solid line: $T=10$ K, dashed line: $T=50$ K, dash-dotted line: $T=70$ K.

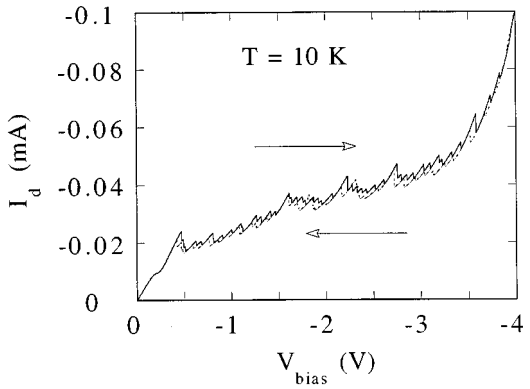

FIG. 3. The dark current–voltage characteristics for increasing bias scan (thick line) and decreasing bias scan (thin line) at $T=10$ K.

both electron coherence length and the value of the internal electric field. This sensitivity is caused by the extended nature of the excited states and by the electron wave interference effect over the neighboring quantum wells.

In a time-independent picture, one can include explicitly the electron coherence length in the calculation of the absorption spectrum by introducing an electron mean free path L_e.[9] The fraction of electrons that are coherent in the process of photon absorption over a distance x in the superlattice is equal to $\kappa\cdot e^{-x/L_e}$, where $\kappa = 1/(\Sigma_{x=x_{\min}}^{x_{\max}} e^{-x/L_e})$ is a normalization constant, and the corresponding absorption is represented by $\alpha(x)$. The term $\alpha(x)$ is calculated assuming electronic wave functions probing the superlattice structure over a distance of x. Because of the electron scattering, quantum wells and the potential distribution beyond this distance will not affect the electronic wave functions in a deterministic manner and they should not lead to any pronounced structure in the absorption spectrum.[10] The overall absorption is thus given by

$$\overline{\alpha}=\sum_{x} \kappa e^{-x/L_e}\alpha(x).$$

Figure 4 shows the calculated absorption spectra at an elec-

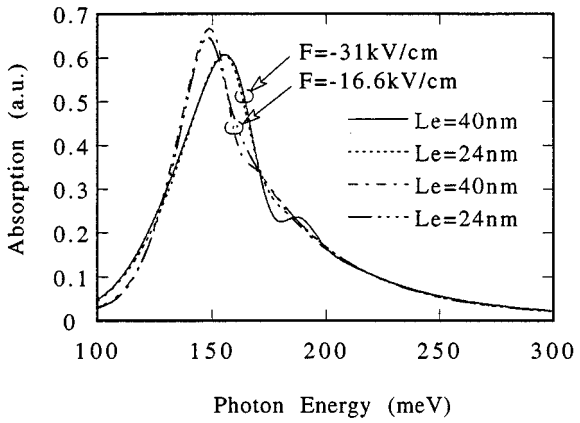

FIG. 4. Theoretical absorption spectra for assumed different electric field in the quantum well structure and different electron coherent length.

tric field of 31 kV/cm, for two assumed different values of electron coherence length. One notices the disappearance of side peaks for short coherence lengths.

The theoretical absorption spectra at different electric fields, and assuming a fixed electron coherent length of 40 nm, are also shown in Fig. 4. It is apparent that the side peak is very weak for low electric fields. To see how these two effects (a change in the electron coherence length or a change in the *internal* electric field) are contributing to the high temperature photocurrent spectra, we consider the $I-V$ characteristics at 70 K (Fig. 2). No appreciable oscillations are evident. The current is dominated by nonresonant tunneling or thermally assisted processes, and there is no sequential resonant tunneling induced EFD formation in the device. The calculated absorption spectra for a uniform electric field of 16.6 kV/cm and two different values of electron coherent length are shown in Fig. 4. The disappearance of the auxiliary peak at 70 K can be explained assuming an electron coherence of length less than 24 nm or a nonuniform electric field distribution in the superlattice.

It is interesting to note that the peak positions in the photocurrent spectra at 70 K have a *voltage dependence* in contrast to the low temperature ones. This is consistent with having no electric field domains in the device. One can see a blueshift of $\sim$1.3 meV, when increasing the bias from -2 to -3 V.

In conclusion, studying the photocurrent spectra and the $I-V$ characteristics of single-bound state MQW structures, the resonant tunneling and EFD formation were analyzed. Evidence for domination of incoherent transport mechanisms at higher temperatures was presented. Electron coherence length shortening and/or electric field nonuniformity in the superlattice are the likely cause for the disappearance of the auxiliary peak in the photocurrent spectra at high temperatures.

This work was supported by the Defense Advanced Research Project Agency (DARPA), and by the Air Force Office of Scientific Research.

[1] L. Esaki and L. L. Chang, Phys. Rev. Lett. **33**, 495 (1974).
[2] F. Capasso, K. Mohammad, and A. Y. Cho, Appl. Phys. Lett. **48**, 478 (1986).
[3] K. K. Choi, B. F. Levine, R. J. Malik, J. Walker, and C. G. Bethea, Phys. Rev. B **35**, 4172 (1987).
[4] Y. Xu, A. Shakouri, and A. Yariv, Appl. Phys. Lett. **66**, 3307 (1995).
[5] J. Kastrup, H. T. Grahn, K. Ploog, F. Prengel, A. Wacker, and E. Scholl, Appl. Phys. Lett. **65**, 1808 (1994).
[6] D. Miller and B. Laikhtman, Phys. Rev. B **50**, 18 426 (1994).
[7] J. S. Blakemore, J. Appl. Phys. **53**, R123 (1982).
[8] L. Thibaudeau, P. Bois, and J. Y. Duboz, J. Appl. Phys. **79**, 446 (1996).
[9] F. Beltram, F. Capasso, D. L. Sivco, A. L. Hutchinson, S.-N. G. Chu, and A. Y. Cho, Phys. Rev. Lett. **64**, 3167 (1990).
[10] A more elaborate analysis may in fact show some extra features in the absorption spectrum originating from the particular nature of a scattering mechanism (e.g., the presence of a threshold energy of 36 meV for polar optical phonon emission in GaAs). Without including these effects, the calculated absorption spectrum matches the experimental photocurrent spectrum very well. This is despite the additional complexity in the photocurrent spectra due to electron emission and capture in quantum wells.